IITRI

GPO PRICE $ _____

CFSTI PRICE(S) $ _____

Hard copy (HC) 3.00

Microfiche (MF) .50

ff 653 July 65

[redacted]

Report No. IITRI-U6003-16
(Quarterly Report)

# INVESTIGATION OF LIGHT SCATTERING IN HIGHLY REFLECTING PIGMENTED COATINGS

National Aeronautics
and Space Administration

IIT RESEARCH INSTITUTE

Report No. IITRI-U6003-16
(Quarterly Report)

# INVESTIGATION OF LIGHT SCATTERING IN HIGHLY REFLECTING PIGMENTED COATINGS

August 1 through November 1, 1965

Contract No. NASr-65(07)
IITRI Project U6003

Prepared by

G. A. Zerlaut, B. H. Kaye
and M. R. Jackson

of

IIT RESEARCH INSTITUTE
Technology Center
Chicago, Illinois 60616

for

National Aeronautics and Space Administration
Office of Advanced Research and Technology
Washington 25, D. C.

Copy No. 93

November 9, 1965

## FOREWORD

This is Report No. IITRI-U6003-16 (Quarterly Report) of IITRI Project U6003, Contract No. NASr-65(07), entitled "Investigation of Light Scattering in Highly Reflecting Pigmented Coatings". This report covers the period from August 1 through November 1, 1965. Previous Quarterly Reports were issued in October 1963, February 1964, May 1964, September 1964, January 1965, March 1965, May 1965, and August 1965. The project is under the technical direction of the Research Projects Laboratory of the George C. Marshall Space Flight Center, and Mr. Daniel W. Gates is project manager.

Because of a divisional reorganization and the accompanying administrative changes, the IITRI number designating this project has been changed from C6018 to U6003. Project administration and technical organization, however, are not affected.

Major contributors to the program include G. A. Zerlaut, project leader; Dr. S. Katz and Dr. B. H. Kaye, theoretical analysis; N. D. Bennett and H. Iglarsh, preparation of random models; and M. R. Jackson, experimental investigator. Experimental data are recorded in logbook C16369.

Respectfully submitted,

IIT RESEARCH INSTITUTE

G. A. Zerlaut
Group Leader
Polymer Research

Approved by:

T. H. Meltzer
Manager
Polymer Research

GAZ/am/jb

ABSTRACT

INVESTIGATION OF LIGHT SCATTERING
IN HIGHLY REFLECTING PIGMENTED COATINGS

12 962

This report is concerned primarily with simulated systems using random-number techniques. Experiments with randomly superimposed screens were performed. Data show that the predicted and measured straight-through fractional areas agree within the limits imposed by experimental error and statistical fluctuations. Thus, the penetration of light into a pigment can be predicted by considering the random screens formed by the pigment in the film.

The use of Monte Carlo simulation techniques resulted in the deduction of a Lambert-Beer equation for the attenuation of light in a pigmented system. A Monte Carlo plotting experiment showed that at 17% pigment by volume, there is an absolute maximum of scattering centers and that further additions of pigment only serve to create larger clusters. Similarly, the Monte Carlo plotting technique was used to explore the possible role of extender pigment in a paint film. The experiment suggests that extender pigments may improve scattering by preventing pigment clusters. The broader implications of the Monte Carlo plotting experiments are discussed.

The significance of specification of particle size is demonstrated. The principal objective is to deduce size distributions of dispersed pigment from the properties of random sections.

Optical experiments are described which demonstrate the ability to investigate the intensity of scattered and transmitted light as a function of angle. The experiments involved the determination of simulated powder mixtures.

Author

TABLE OF CONTENTS

## LIST OF TABLES

LIST OF FIGURES

# INVESTIGATION OF LIGHT SCATTERING IN HIGHLY REFLECTING PIGMENTED COATINGS

## I. INTRODUCTION

The objective of this program is the application of light-scattering theories to polydisperse, highly reflecting, highly pigmented coatings. The program is aimed at a definition of the light-scattering parameters associated with the maximum reflection of solar radiation. The definition of these factors should facilitate the eventual development of more efficient solar reflectors and, perhaps more important, may extend the applications of light-scattering theory to the solution of other problems.

Previous work has involved (1) a review of classical light-scattering theory with emphasis on that portion having the most promise for application to multiple scattering events, (2) the generation of data on the optical properties of carefully prepared arrays of silver bromide particles dispersed in gelatin, and (3) the conception of theoretical approaches and random-walk techniques with which to treat the problem of multiple scattering.

The adaptation of classical Mie theory to multiple scattering has been discussed in several of the previous Quarterly Reports. This report does not contain a discussion of classical Mie theory; the final review of classical light-scattering theory will be given in the next report.

The experimental investigation of the optical properties of silver bromide arrays has been completed. The results of these studies as well as the comprehensive analysis of classical theory in terms of multiple scattering phenomena are expected to aid in the adaptation of Monte Carlo techniques to the multiple interaction problem.

The Monte Carlo investigations discussed in the last two reports, (Reports No. IITRI-C6018-14 and IITRI-C6015-15), have been expanded and intensified accordingly. Indeed, the technique as it now exists is capable of generating considerable quantities of information. This report therefore not only continues these discussions but also attempts to elucidate several applied sciences (as well as paint technology) that may benefit from these investigations.

## II. SIMULATED SYSTEMS USING RANDOM-NUMBER TECHNIQUES

### A. Some Properties of Random Systems: Randomly Superimposed Screens

Experiments in which the residual straight-through path for a system of randomly superimposed screens was simulated by using Xerox copies of screen diagrams were detailed in the last report. During this report period the work was extended to the investigation of the straight-through path for three, four, and five randomly superimposed screens.

Figures 1 and 2 show typical simulated systems for four and five screens, and Table 1 summarizes the experimental results.

The data show that the predicted and measured straight-through fractional areas agree within the limits imposed by experimental error and statistical fluctuations. This agreement indicates that the penetration of a light beam into a pigment can be predicted by considering the random screens formed by the pigment in the paint film. Laboratory experiments will be carried out with pigmented films to determine whether the theory can be applied directly to paint films.

### B. Simulation of the Penetration of a Plane Parrallel Beam of Incoherent Light through a Rain Cloud

#### 1. Simulation of the Cloud

The penetration of radiation into a rain cloud and the probabilities of secondary scattering within the cloud were discussed previously (Report No. C6018-13). For a complete random-walk treatment of energy penetration through a cloud of

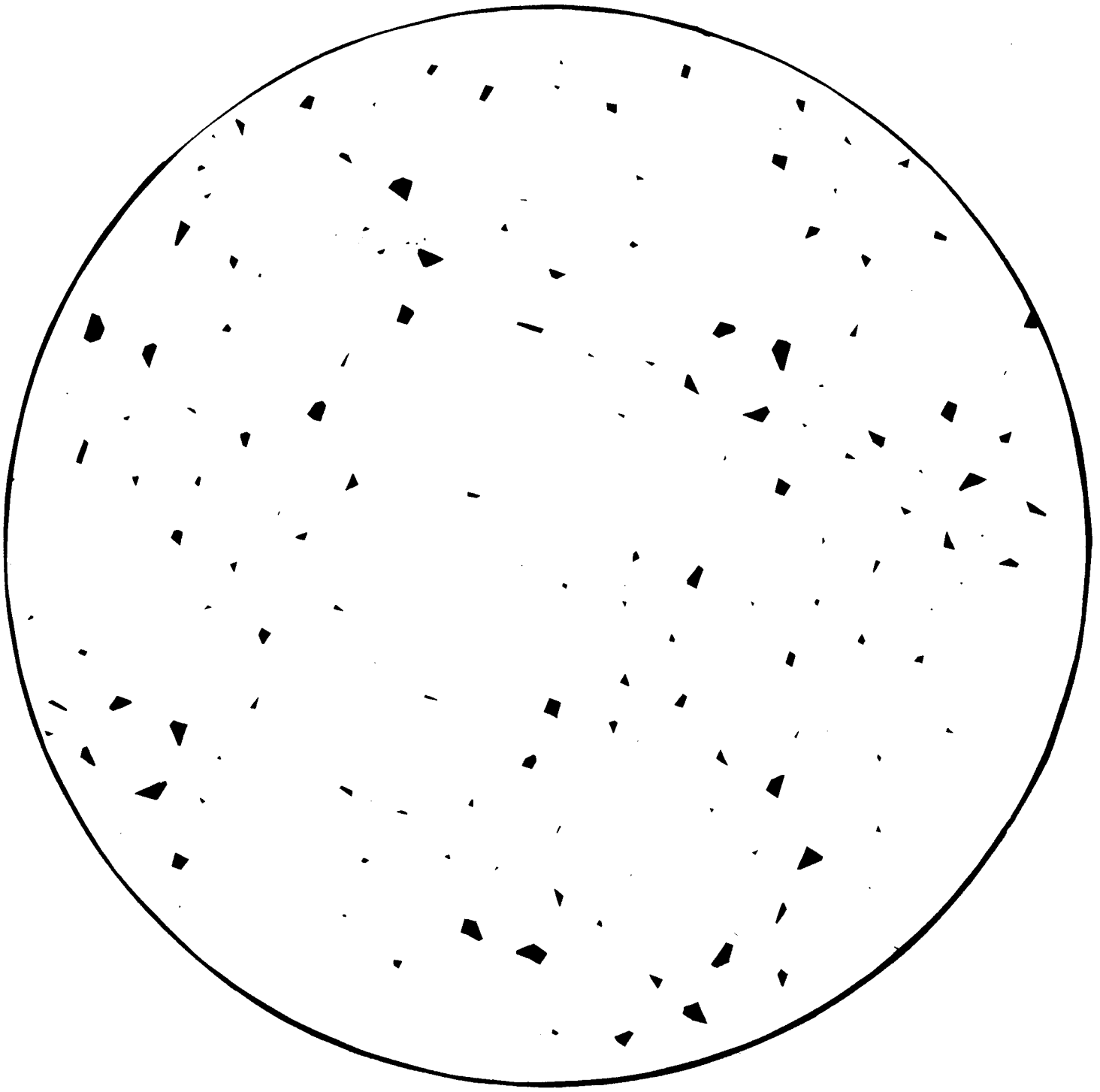

FIG. 1 RESULTANT STRAIGHT-THROUGH AREA FOR 4 RANDOMLY SUPERIMPOSED SCREENS

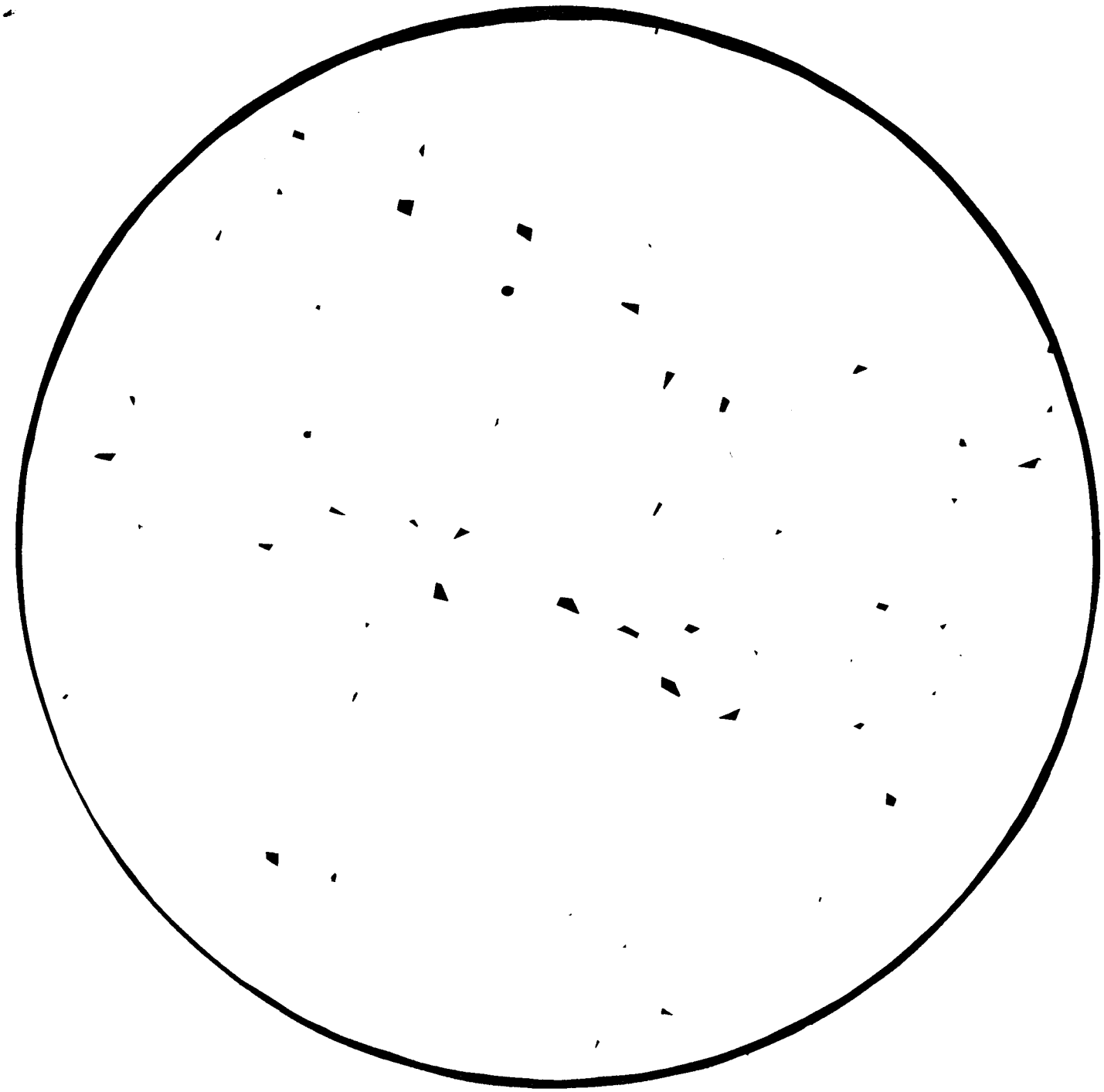

FIG. 2 RESULTANT STRAIGHT - THROUGH AREA FOR 5 RANDOMLY SUPERIMPOSED SCREENS

Table 1

AVAILABLE STRAIGHT-THROUGH PATHS
IN RANDOMLY SUPERIMPOSED SCREENS
(Open Space in Original Screen = 0.303 of Total Area)

| Number of Screens Superimposed | Straight-Through Fractional Area | |
|---|---|---|
| | Predicted | Measured |
| 2 | 0.092 | 0.092 |
| | | 0.102 |
| | | 0.098 |
| | | 0.101 |
| | | 0.105 |
| 3 | 0.028 | 0.030 |
| | | 0.028 |
| 4 | 0.008 | 0.012 |
| | | 0.011 |
| | | 0.007 |
| | | 0.010 |
| | | 0.008 |
| | | 0.006 |
| | | 0.014 |
| 5 | 0.002 | 0.003 |
| | | 0.001 |
| | | 0.001 |
| 6 | 0.0006 | Too small to measure. |

randomly distributed particles, the probabilities of the persistence of the forward beam have to be known. When these probabilities have been determined, the energy flux at any surface perpendicular to the direction of the original energy flow at a certain depth can be described by the equation

$$E_T = E_O \cdot P_{(x)} + E_D \qquad (1)$$

where $E_T$ is the total energy

$E_O$ is the original energy in parallel forward beam

$P_{(x)}$ is the probability of persistence at depth x

$E_D$ is the diffuse energy flux

Several problems arise in predicting the decay of the forward energy beam. First, although formulas for light-scattering phenomena are useful in predicting the total energy removed from the forward direction, it is not easy (sometimes it is impossible) to determine the area of the wave front distributed by the particle. The second major problem is to predict the statistics of persistence of the forward beam. For instance, how many particles are effective scattering centers, and what is the probability that particles along the direction of traverse will occur in line with particles nearer to the source? The following experiment was devised to study this type of problem.

Consider a rectangular grid. Along the x-axis let there be $N_x$ units, and along the y-axis $N_y$ units. Therefore within the major grid there are $N_x N_y$ small squares. If we now consider

the path of a plane parallel beam of light passing through the plane of the grid, the z-axis perpendicular to the plane of the grid represents the direction of travel. If an observer looked along the z-axis and if a cloud of particles was placed between the observer and the source of light, the observer would not be aware of the z coordinate of the particles. The projected representation of the cloud on the x-y plane would represent the appearance of the cloud to the distant observer. Also, the fraction of open area seen by the observer would represent the fraction of the initial forward beam penetrating the cloud if diffraction effects were negligible.

Therefore the following series of experiments was conducted to simulate the appearance of a cloud of monosized particles. A piece of graph paper with 70 units along the y-axis and 100 units along the x-axis was selected. A pair of coordinates was selected from random-number tables, and the appropriate square on the grid was filled with black ink. This blacked-out square represents the shadow of the particle. If the particles are small, the square will have to represent its effective area*; if the particles are large, the square will be their geometric shadow. It can be argued that the use of square particles that cannot partially overlap (only completely or not at all) is a very artificial system. It is artificial, but the generalizations that are reached from this study are very informative and probably

*The exact meaning of effective depends upon the system considered and is not defined further at this stage.

qualitatively correct. After all, the simple kinetic theory of gases is artificial, but it served as a useful tool in the development of physical science.

In this preliminary study we will first consider particles larger than the wavelength of light such that only the geometric shadow needs to be considered. In order to simulate the light-obscuring behavior of a cloud particle, the appropriate number of particles are plotted on the grid. Typical sets of coordinates selected from random-number tables are given in Table 2. When coordinates occur for a position that is already occupied, this represents a particle that is ineffective in destroying the forward beam. The fact that an overlapped particle has occurred is recorded, and plotting continues. The number of particle coordinates selected represents the concentration of particles in the beam, and the number of spaces remaining represents the open area persisting. Therefore a record of the two numbers simulates the efficiency with which the forward beam is diverted.

Table 2

TYPICAL SETS OF COORDINATES
USED IN THE MONTE CARLO SIMULATION
OF PARTICLE-SCATTERING PHENOMENA

| x Coordinate | y Coordinate |
|---|---|
| 7 | 33 |
| 71 | 21 |
| 30 | 24 |
| 75 | 21 |
| 76 | 47 |
| 14 | 18 |
| 47 | 53 |

Table 2 (cont.)

TYPICAL SETS OF COORDINATES
USED IN THE MONTE CARLO SIMULATION
OF PARTICLE-SCATTERING PHENOMENA

| x Coordinate | y Coordinate |
|---|---|
| 67 | 29 |
| 80 | 61 |
| 94 | 43 |

The blocking out of the squares selected by random-number coordinates is an abstract simulation of several other systems of interest to the investigation of the performance of a paint, so that the buildup of particles in the grid was very carefully recorded. All coordinates were recorded, and each pair of coordinates that represented an overlapped particle was marked with an asterisk. Each time the plotting of 70 coordinates was completed, the grid was examined visually for squares that were touching, and the number of squares within any cluster of profiles was recorded.

Since this information will be referred to extensively, the record of the number of overlapped particles is given in complete form in Table 3. For this initial experiment the number of particles plotted was terminated when the number of squares that were blocked out represented 20% of the area of the original grid. If necessary, the experiment can be continued easily, but a great deal of information was already available at this stage, and it was deemed more efficient to digest this information

Table 3

OVERLAPPED PARTICLES IN MONTE CARLO EXPERIMENT

| Number of Pairs of Coordinates | Overlapping Particles | Open Area Units |
|---|---|---|
| 70 | 0 | 6.930 |
| 140 | 0 | 6.860 |
| 210 | 3 | 6.793 |
| 280 | 6 | 6.726 |
| 350 | 10 | 6.660 |
| 420 | 15 | 6.595 |
| 490 | 20 | 6.530 |
| 560 | 32 | 6.472 |
| 630 | 35 | 6.405 |
| 700 | 42 | 6.342 |
| 770 | 49 | 6.279 |
| 840 | 56 | 6.216 |
| 910 | 62 | 6.152 |
| 980 | 66 | 6.086 |
| 1050 | 76 | 6.026 |
| 1120 | 90 | 5.970 |
| 1190 | 105 | 5.915 |
| 1260 | 113 | 5.853 |
| 1330 | 127 | 5.797 |
| 1400 | 145 | 5.745 |
| 1470 | 156 | 5.686 |
| 1540 | 172 | 5.632 |
| 1590 | 180 | 5.600 |

before continuing the experiment.

The information on the buildup of cluster is given in Table 4. The master plot of the squares on the grid is shown in Figure 3 and a typical selection of the clusters is shown in Figure 4. The various implications of the data are discussed below.

2. Rate of Overlapping within the Simulated Cloud (Lambert-Beer Law Simulation)

Increasing the number of pairs of coordinates considered for plotting on the master grid is equivalent to two physical procedures. First, it is equivalent to studying the changes in attenuation for a unit volume of the beam as the concentration increases. Alternatively, it could be equivalent to studying the increased attenuation caused by increasing the path length through a constant volume concentration cloud.

Consider what has happened when N pairs of coordinates have been selected; this is equivalent to considering the effect of N particles. Let there be $\emptyset$ unit squares at the commencement of the plotting experiment. Let the number of particles that have overlapped be given by $\beta$. The original energy of the beam is $\emptyset \cdot E$, where E is the energy per unit square. The energy passing through the cloud is given by the expression:

$$\left[\emptyset - (N - \beta)\right]E$$

Let the incident energy be denoted by the term $I_0$, and the transmitted energy by $I_T$, then

$$\frac{I_T}{I_0} = \frac{(\emptyset - N + \beta)}{\emptyset} = \zeta \qquad (2)$$

Table 4

BUILDUP OF CLUSTERS ON GRID IN MONTE CARLO EXPERIMENT

| Number of Pairs of Coordinates | Number of Overlapping Particles | Number of Units in Cluster Number of Clusters | | | | | | | | | | | | | | | |
|---|---|---|---|---|---|---|---|---|---|---|---|---|---|---|---|---|---|
| | | 2 | 3 | 4 | 5 | 6 | 7 | 8 | 9 | 10 | 11 | 12 | 13 | 14 | 15 | 16 | 17 |
| 140 | 0 | 8 | | | | | | | | | | | | | | | |
| 210 | 3 | 16 | 1 | | | | | | | | | | | | | | |
| 280 | 6 | 29 | 3 | | | | | | | | | | | | | | |
| 350 | 10 | 38 | 6 | | | | | | | | | | | | | | |
| 420 | 15 | 52 | 7 | 3 | 1 | | | | | | | | | | | | |
| 490 | 20 | 65 | 16 | 3 | 2 | | | | | | | | | | | | |
| 560 | 32 | 76 | 21 | 5 | – | 2 | | | | | | | | | | | |
| 630 | 35 | 77 | 23 | 5 | 4 | 4 | 1 | | | | | | | | | | |
| 700 | 42 | 82 | 31 | 4 | 5 | 5 | 2 | | | | | | | | | | |
| 770 | 49 | 82 | 38 | 9 | 3 | 8 | 3 | | | | | | | | | | |
| 840 | 56 | 86 | 43 | 15 | 7 | 6 | 4 | 0 | 1 | | | | | | | | |
| 910 | 62 | 90 | 46 | 21 | 8 | 5 | 4 | 2 | 1 | 1 | | | | | | | |
| 980 | 66 | 97 | 49 | 24 | 8 | 5 | 2 | 6 | 2 | 0 | 1 | | | | | | |
| 1050 | 76 | 98 | 54 | 20 | 11 | 10 | 2 | 3 | 4 | 0 | 2 | 1 | | | | | |
| 1120 | 90 | 105 | 56 | 20 | 13 | 6 | 5 | 4 | 5 | 1 | 1 | 0 | 1 | 1 | | | |
| 1190 | 105 | 96 | 54 | 24 | 16 | 7 | 6 | 5 | 5 | 3 | 2 | 0 | 1 | 1 | | | |
| 1260 | 113 | 100 | 55 | 27 | 18 | 10 | 6 | 3 | 6 | 4 | 3 | 0 | 0 | 1 | 1 | | |
| 1330 | 127 | 96 | 58 | 28 | 19 | 15 | 8 | 3 | 6 | 2 | 3 | 1 | 1 | 1 | 0 | 1 | |
| 1400 | 145 | 95 | 57 | 25 | 21 | 15 | 12 | 3 | 7 | 2 | 3 | 1 | 0 | 2 | 2 | 1 | |
| 1470 | 156 | 90 | 64 | 23 | 13 | 19 | 17 | 2 | 7 | 7 | 3 | 1 | 0 | 3 | 2 | 1 | |
| 1540 | 172 | 92 | 65 | 23 | 15 | 19 | 16 | 2 | 9 | 5 | 7 | 2 | 0 | 1 | 3 | 2 | |
| 1580 | 180 | 89 | 58 | 23 | 20 | 18 | 16 | 4 | 9 | 6 | 4 | 2 | 0 | 2 | 3 | 2 | 1[a] |

[a]Also 1 at 21.

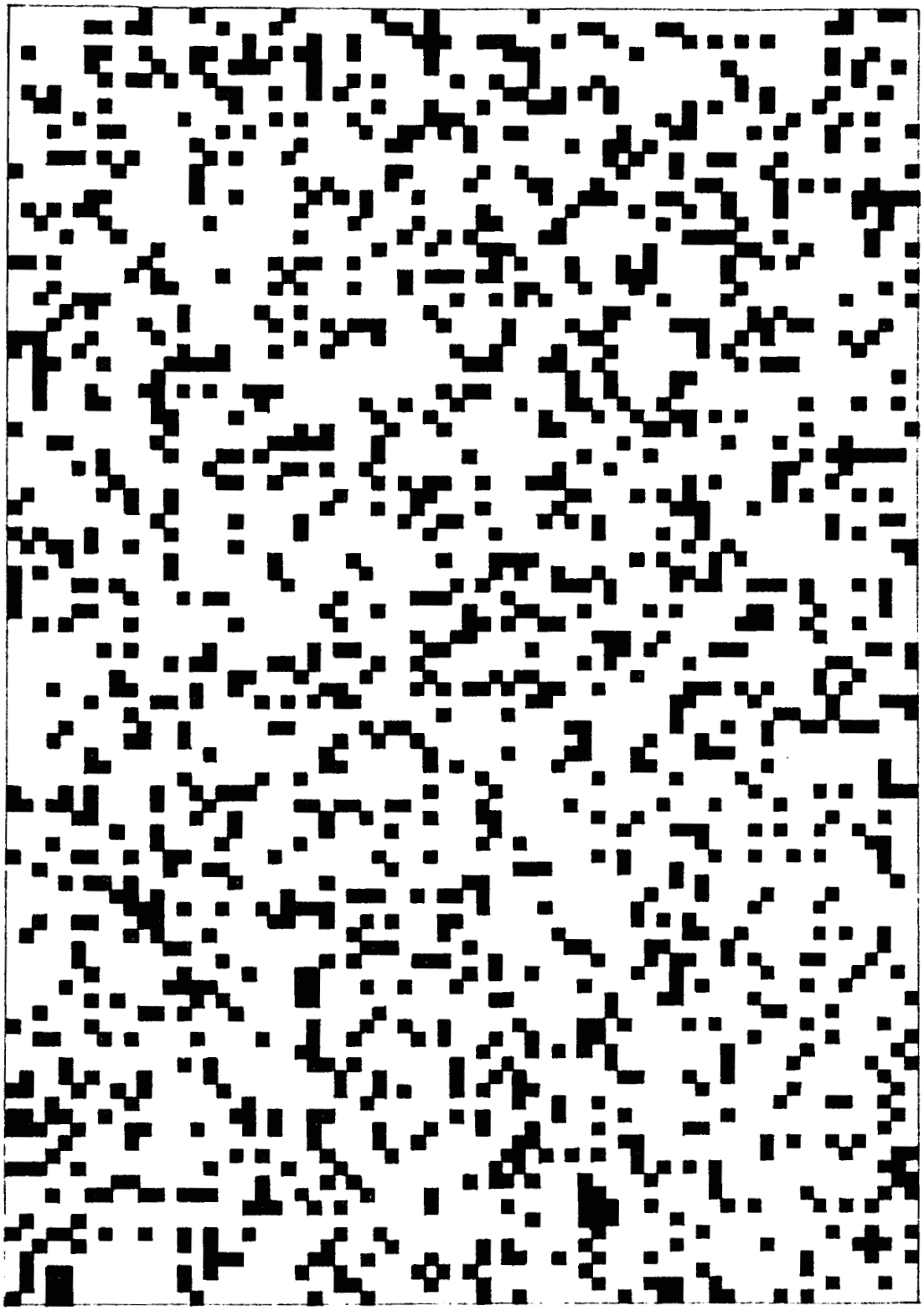

FIG. 3 MASTER PLOT OF PARTICLES IN THE X,Y, PLANE

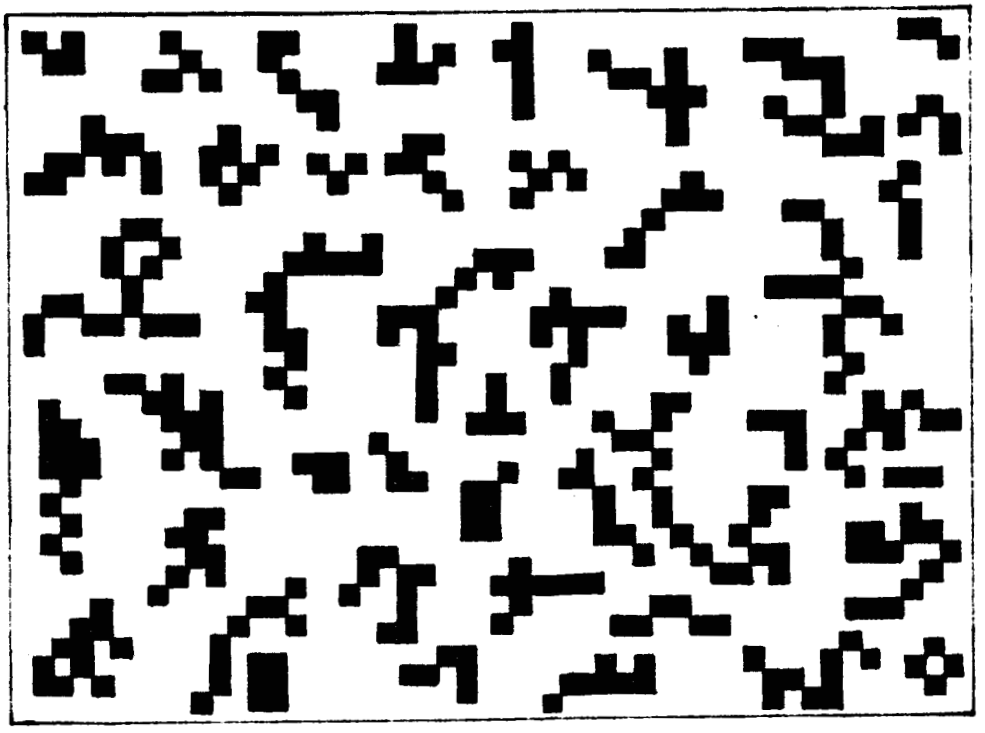

FIG. 4 CLUSTERS FORMED AT 20% COVERAGE

when $\delta$ denotes the fractional area remaining open.

It has been established empirically that the ratio of the incident to the transmitted energy for light passing through a dilute cloud is given by the Lambert-Beer Law. This law can conveniently be written in the form

$$\log \frac{I_T}{I_0} = \exp(-KC\ell) \tag{3}$$

where K is a constant dependent on the size and geometry of the particle, $\ell$ is the length of the beam's path considered, and C is the concentration of a unit volume of the cloud. The product $C\ell$ represent the total number of particles in a unit area.

Therefore the Lambert-Beer Law can be written in the form

$$\log \frac{I_T}{I_0} = A + N \tag{4}$$

where A is a constant.

If the simulation experiment is in agreement with empirically determined knowledge, then, from Equations 2 and 4,

$$\log \delta = B + N \tag{5}$$

where B is an arbitary constant.

That is, a plot of the logarithm of $\delta$ against N should be a straight line. The relevant information abstracted from Table 3 has been plotted in Figure 5. These data follow the predicted pattern, demonstrating that a Lambert-Beer equation for the attenuation of a light beam can be deduced from statistical reasoning alone. The physical significance of this information is being explored.

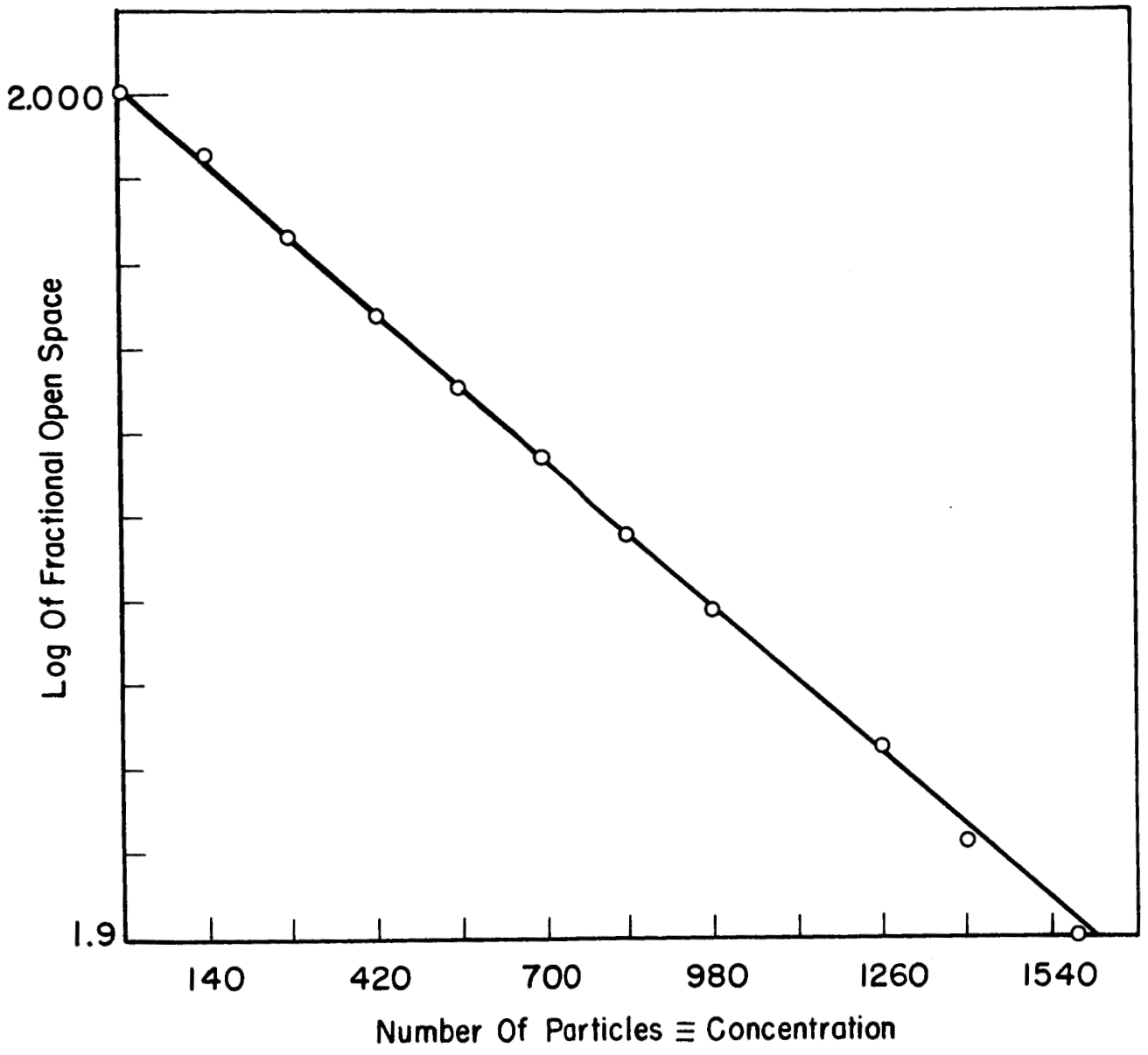


FIG. 5 PLOT OF LOGARITHM OF FRACTIONAL OPEN SPACE AGAINST TOTAL NUMBER OF PARTICLES

C. Interpretation of the Monte Carlo Grid-Plotting Experiment

The basic grid of the Monte Carlo experiment can be considered a thin section through a paint film in which monosized particles are dispersed. The section is one unit thick, and the particles are located exactly in the plane of the section. Again, although this is an idealized paint system, the information derived from it is probably qualitatively correct. For this interpretation of the plotting experiments, the overlapped particles are regarded as particles that try to occupy positions already filled. They are not considered in studying the distribution of particles in the film section since they represent nonpermissible particles.

Therefore, the important parameter for this study is N', the number of spaces occupied. It would seem reasonable to regard the cluster as the scattering unit. In fact, it has generally been assumed in paint publications that a badly dispersed pigment has low scattering efficiency because the effective pigment particles are larger and therefore less effective.

Let us consider the case of a pigment dispersed by random forces that act at high shear rates in a viscous medium. When the shearing forces cease, the dispersion acheived is regarded as fixed, because particle movement will normally be negligible in a highly viscous medium. Plotting the blackened squares corresponds physically to the random positioning of the particles. The appearance of the grid at progressively increasing numbers of particles plotted therefore corresponds to the appearance of the film at increasing concentrations.

The following information can be abstracted from Table 4. If we treat a cluster as the scattering unit, we can calculate S, which is the total number of scatterers in the paint film at each volume concentration. We note that the volume concentration and surface exposed are numerically equal. The data in this form are summarized in Table 5. In Figure 6 the number of scatterers achieved is expressed as a fraction of the number of particles placed in the section. This curve offers a statistical explanation of the fact that the higher the volume concentration of the pigment dispersion, the lower the hiding power of a given amount of pigment.

If, instead of plotting percentage scattering centers, we plot the absolute number of scattering units per unit volume at various volume concentrations, the data appears as shown in Figure 7. Note that at 17% by volume there is an absolute maximum of scattering centers and that further additions of pigment particles only serve to create larger clusters. This suggests the possibility that there is an optimum pigment volume concentration at which maximum numbers of scatters per unit volume are achieved. A preliminary survey of the literature indicates that this statistical reasoning may offer an explanation of the experimentally determined peak in the scattering

Table 5

CLUSTER FORMATION DATA FOR MONTE CARLO EXPERIMENT

| Particles (N') | Fraction (u) | Number of Clusters: Number of Units in Cluster | | | | | | | | | | | | | | | | Number of Independent Scattering Centers (S) |
|---|---|---|---|---|---|---|---|---|---|---|---|---|---|---|---|---|---|---|
| | | 1 | 2 | 3 | 4 | 5 | 6 | 7 | 8 | 9 | 10 | 11 | 12 | 13 | 14 | 15 | 16 | 17 | |
| 140 | 0.020 | 128 | 8 | | | | | | | | | | | | | | | | 132 |
| 207 | 0.030 | 172 | 16 | 1 | | | | | | | | | | | | | | | 189 |
| 274 | 0.039 | 207 | 29 | 3 | | | | | | | | | | | | | | | 239 |
| 340 | 0.048 | 246 | 38 | 6 | | | | | | | | | | | | | | | 292 |
| 405 | 0.058 | 263 | 52 | 7 | 3 | 1 | | | | | | | | | | | | | 325 |
| 470 | 0.067 | 270 | 65 | 16 | 3 | 2 | | | | | | | | | | | | | 356 |
| 528 | 0.075 | 281 | 76 | 21 | 5 | - | 2 | | | | | | | | | | | | 385 |
| 595 | 0.085 | 301 | 77 | 23 | 5 | 4 | 2 | 1 | | | | | | | | | | | 415 |
| 658 | 0.094 | 316 | 82 | 31 | 4 | 5 | 5 | 2 | | | | | | | | | | | 445 |
| 721 | 0.103 | 323 | 82 | 38 | 9 | 3 | 8 | 3 | | | | | | | | | | | 466 |
| 784 | 0.112 | 315 | 86 | 43 | 15 | 7 | 6 | 4 | 0 | 1 | | | | | | | | | 477 |
| 848 | 0.121 | 313 | 90 | 46 | 21 | 8 | 5 | 4 | 2 | 1 | 1 | | | | | | | | 991 |
| 914 | 0.131 | 316 | 97 | 49 | 24 | 8 | 5 | 2 | 6 | 2 | 0 | 1 | | | | | | | 509 |
| 974 | 0.138 | 313 | 98 | 54 | 20 | 11 | 10 | 2 | 3 | 4 | 0 | 2 | 1 | | | | | | 518 |
| 1030 | 0.147 | 311 | 105 | 56 | 20 | 13 | 6 | 5 | 4 | 5 | 1 | 1 | 0 | 1 | 1 | | | | 529 |
| 1085 | 0.155 | 307 | 96 | 54 | 24 | 16 | 7 | 6 | 5 | 5 | 3 | 2 | 0 | 1 | 1 | | | | 528 |
| 1147 | 0.161 | 302 | 100 | 55 | 27 | 18 | 10 | 6 | 3 | 6 | 4 | 3 | 0 | 0 | 1 | 1 | | | 536 |
| 1203 | 0.172 | 298 | 96 | 58 | 28 | 19 | 15 | 8 | 3 | 6 | 2 | 3 | 1 | 1 | 1 | 0 | 1 | | 540 |
| 1255 | 0.179 | 289 | 95 | 57 | 25 | 21 | 15 | 12 | 3 | 7 | 2 | 3 | 1 | 0 | 2 | 2 | 1 | | 534 |
| 1314 | 0.188 | 270 | 90 | 64 | 23 | 13 | 19 | 17 | 2 | 7 | 7 | 3 | 1 | 0 | 3 | 2 | 1 | | 520 |
| 1368 | 0.195 | 262 | 92 | 65 | 23 | 15 | 19 | 16 | 2 | 9 | 5 | 7 | 2 | 0 | 1 | 3 | 2 | | 523 |
| 1400 | 0.200 | 252 | 89 | 58 | 23 | 20 | 18 | 16 | 4 | 9 | 6 | 4 | 2 | 0 | 2 | 3 | 2 | 1[a] | 510 |

[a]Plus one cluster of 21 units.

Note: u = corresponding volume fraction when N' particles have been plotted.
S = number of independent scattering centers at each value of u.

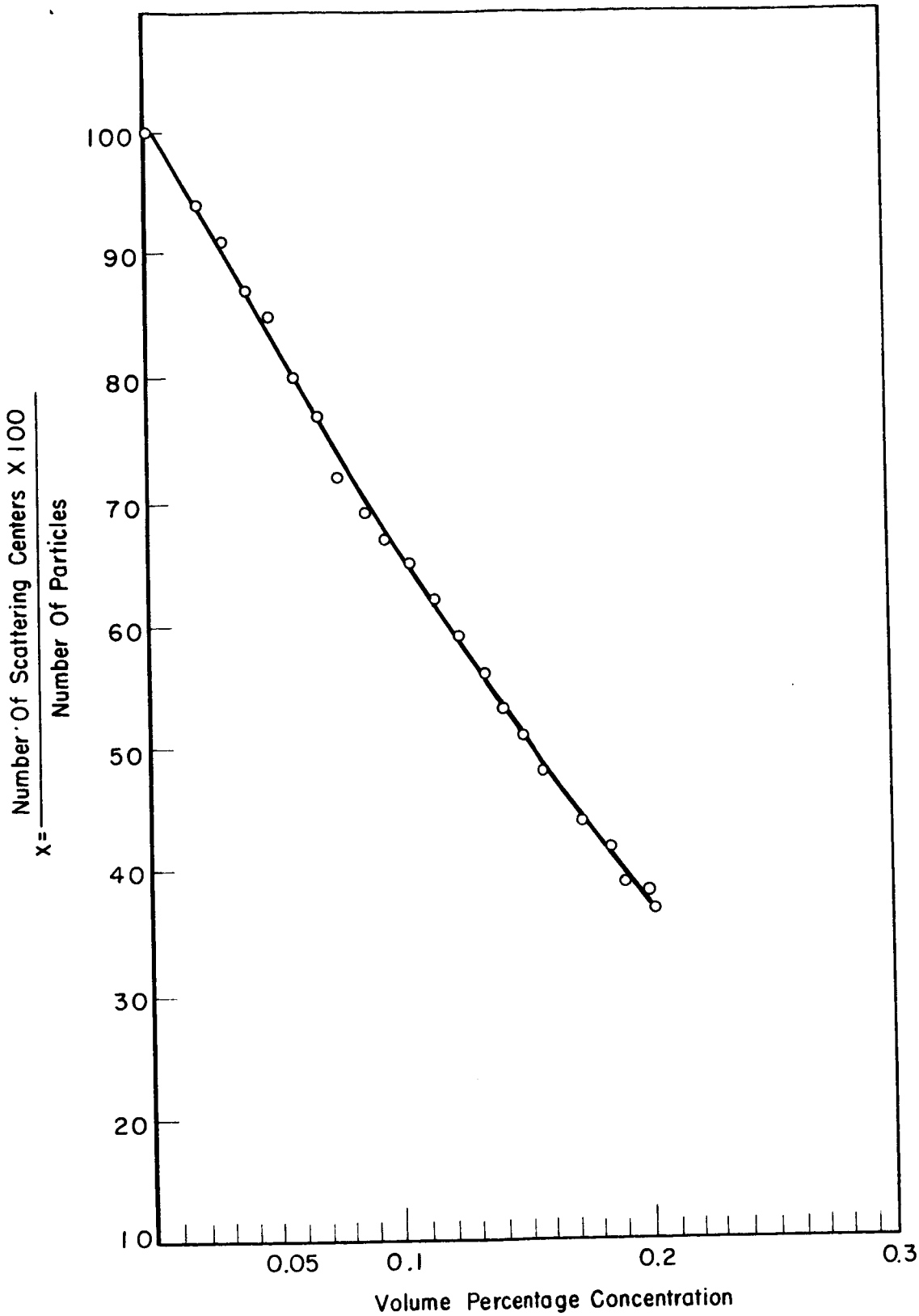


FIG.6 NUMBER OF SCATTERING CENTERS EXPRESSED AS A PERCENTAGE OF TOTAL NUMBER OF PARTICLES AT VARIOUS VOLUME CONCENTRATIONS FOR RANDOMLY DISTRIBUTED MONOSIZED PARTICLES

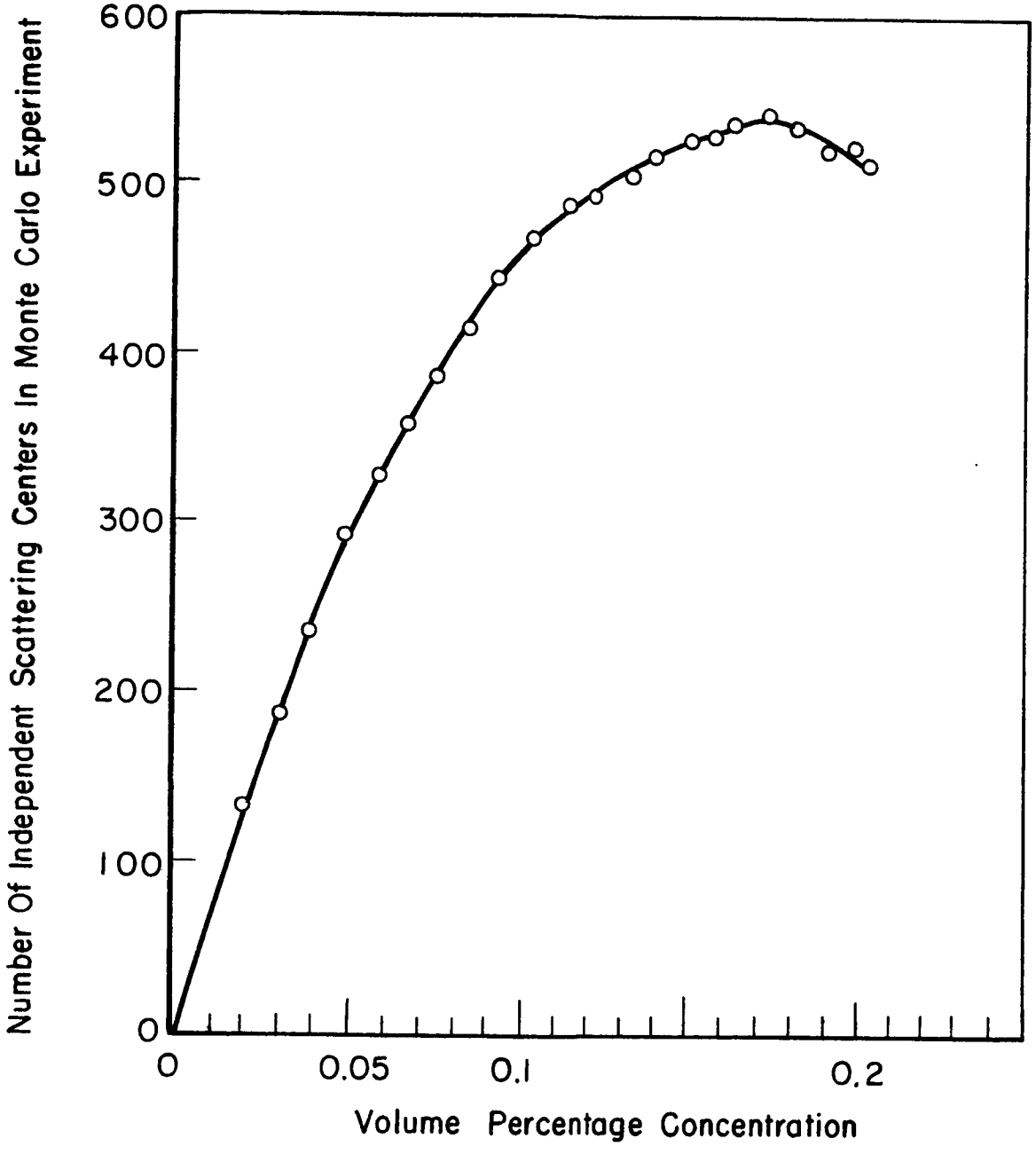


FIG. 7 ABSOLUTE NUMBER OF SCATTERING CENTERS PER UNIT VOLUME

power/PVC relationships for paints that have been discussed by several investigators.[1-3] The search for relavent published experimental data on this topic is continuing and, if necessary, additional experimental verification will be sought.

If the growth of the different sized clusters is plotted (Figure 8), the reason for the drop in the scattering centers achieved with rising concentration is confirmed; i.e., further addition of particles creates bigger clusters and fewer scattering centers. Thus the number of doublets initially increases at a rapid rate and then declines as further single particles convert doublets into triplets.

D. Simulated Pigment-Extender Paint System

A simple modification of the original Monte Carlo plotting experiment can be used for exploring the possible role of extender particles in a paint film. Consider an idealized system in which equal quantities of equally sized pigment and extender particles are randomly dispersed. To simulate such a system we carry out the following transformation by using the master grid of Figure 3.

A transparent piece of graph paper is placed on top of the finished plotted system. In a random-number table odd and even

---

[1] Steig, F. B., Jr., Off. Digest, Federation of Paint and Varnish Production Clubs, 29, No. 388, 439 (May 1957)

[2] Armstrong, W. G., and Madson, W. H., Ind. Eng. Chem., 39, 944(1947)

[3] Zerlaut, G. A., "Utilization of Pigmented Coatings for the Control of Equilibrium Skin Temperatures of Space Vehicles", Proceedings, Aerospace Finishing Symposium, Fort Worth, Texas, December 8, 9, 1959

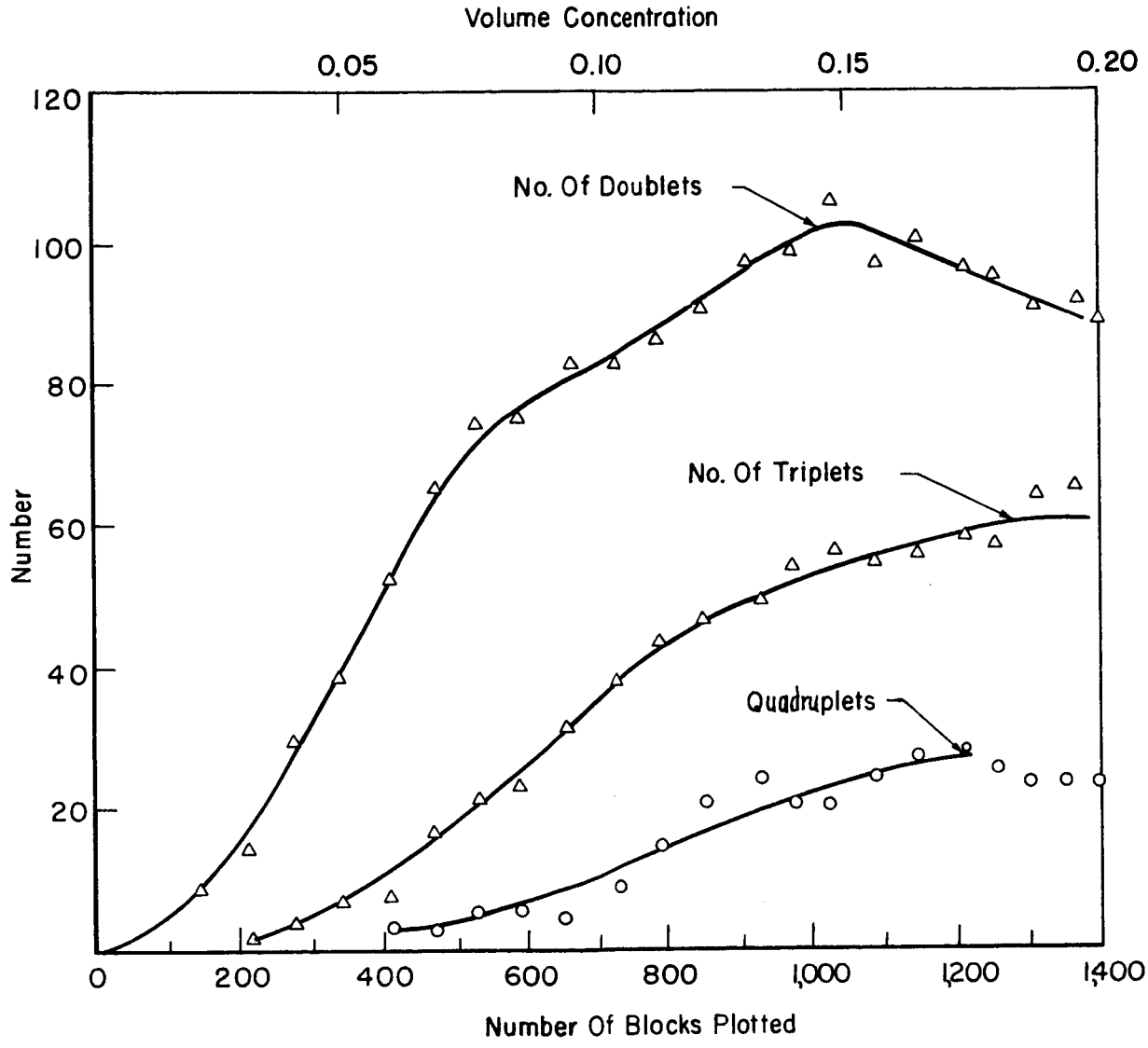


FIG. 8 NUMBER OF DIFFERENT SIZED CLUSTERS AT VARIOUS VOLUME CONCENTRATION FOR MONOSIZED BLOCK MONTE CARLO EXPERIMENT

numbers occur equally. Therefore if each particle is marked through onto the new graph paper in conjunction with a random-number table -- marking ◘ for an even number and o for an odd number in the random number table, then the resultant system represents what would be obtained for equal numbers of pigment and extender particles. The ◘ denotes pigment and o the extender particles.

The resultant transformation, corresponding to 790 particles plotted, is shown in Figure 9. The original data (for the pigment alone, Table 5) were obtained when 784 particles were plotted. The number of particles plotted in each case is sufficiently close for comparison of the number and type of scattering centers achieved for a fixed volume concentration with and without extender particles. For direct comparison, Table 6 lists the cluster distribution for the pigment plus extender (abstracted from Figure 9) and that for the pigment alone (from Table 5).

Table 6

DATA ON CLUSTER FORMATION AT 0.10 VOLUME FRACTION OF IDEALIZED MONOSIZED PIGMENT DISPERSED WITH AND WITHOUT THERORETICAL EXTENDER

| Pigment | Number of Particles, N' | Number of Clusters: Number of Units in Cluster 1 | 2 | 3 | 4 | 5 | 6 | 7 | 8 | 9 | Number of Independent Scattering Centers, S |
|---|---|---|---|---|---|---|---|---|---|---|---|
| Alone | 784 | 315 | 86 | 43 | 15 | 7 | 6 | 4 | - | 1 | 477 |
| Plus extender | 790 | 387 | 75 | 45 | 15 | 6 | 1 | 2 | 1 | - | 532 |

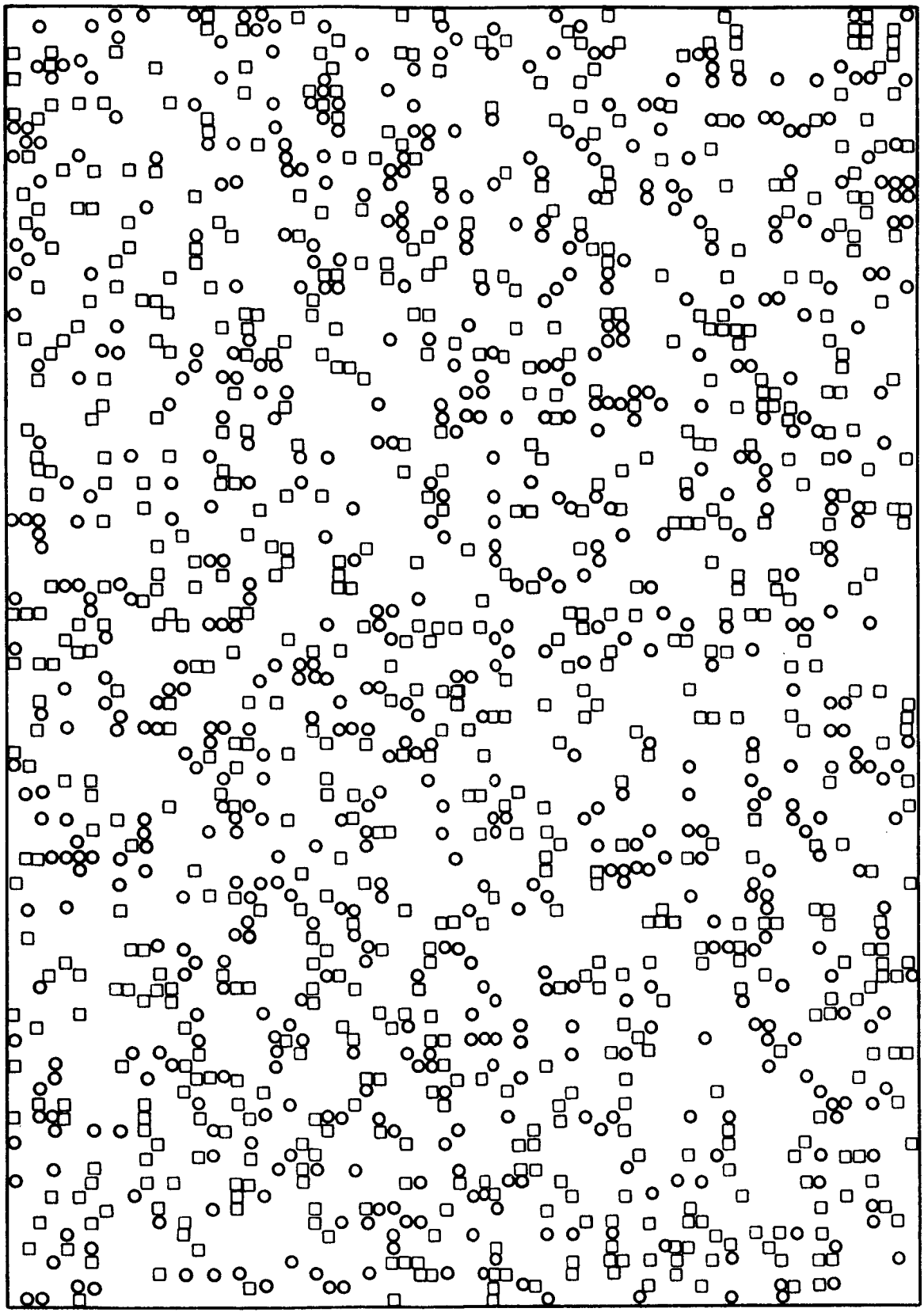

FIG. 9 SIMULATED PIGMENT — EXTENDER SYSTEM

The data in Table 6 show that when an extender is present, (1) there is an overall increase of 12% in the number of scattering achieved, (2) there is a 23% increase in the number of single-particle centers (these which are probably the most effective in scattering the light), and (3) the overall number of scattering centers is as high as the total number achieved at any higher concentration with the pigment alone (Figure 3).

When the cluster distributions for both pigments (with and without extender) are plotted (Figure 10), both obey the log-normal distribution. Figure 10 also shows that when an extender is present, there is less porbability that the larger clusters will occur.

This simulation experiment suggests strongly that the extender has a definite role in light-scattering phenomena, i.e., in preventing pigment clusters by mechanical competition for possible positions. Note that an encapsulated pigment would carry its own "built-in" extender, i.e., it would have a region surrounding it that another pigment particle could not occupy; thus it could be a very efficient light-scattering center in a paint film.

## E. Implication of Monte Carlo Experiment for Air Pollution Studies

An important problem to be overcome in the assessment of the material deposited on filter paper or a microscope slide is the amount of overlapping that occurs as the particles are being deposited. (Report No. IITRI-C6018-15). The Monte Carlo plotting experiment can be regarded as the simulation of the successive

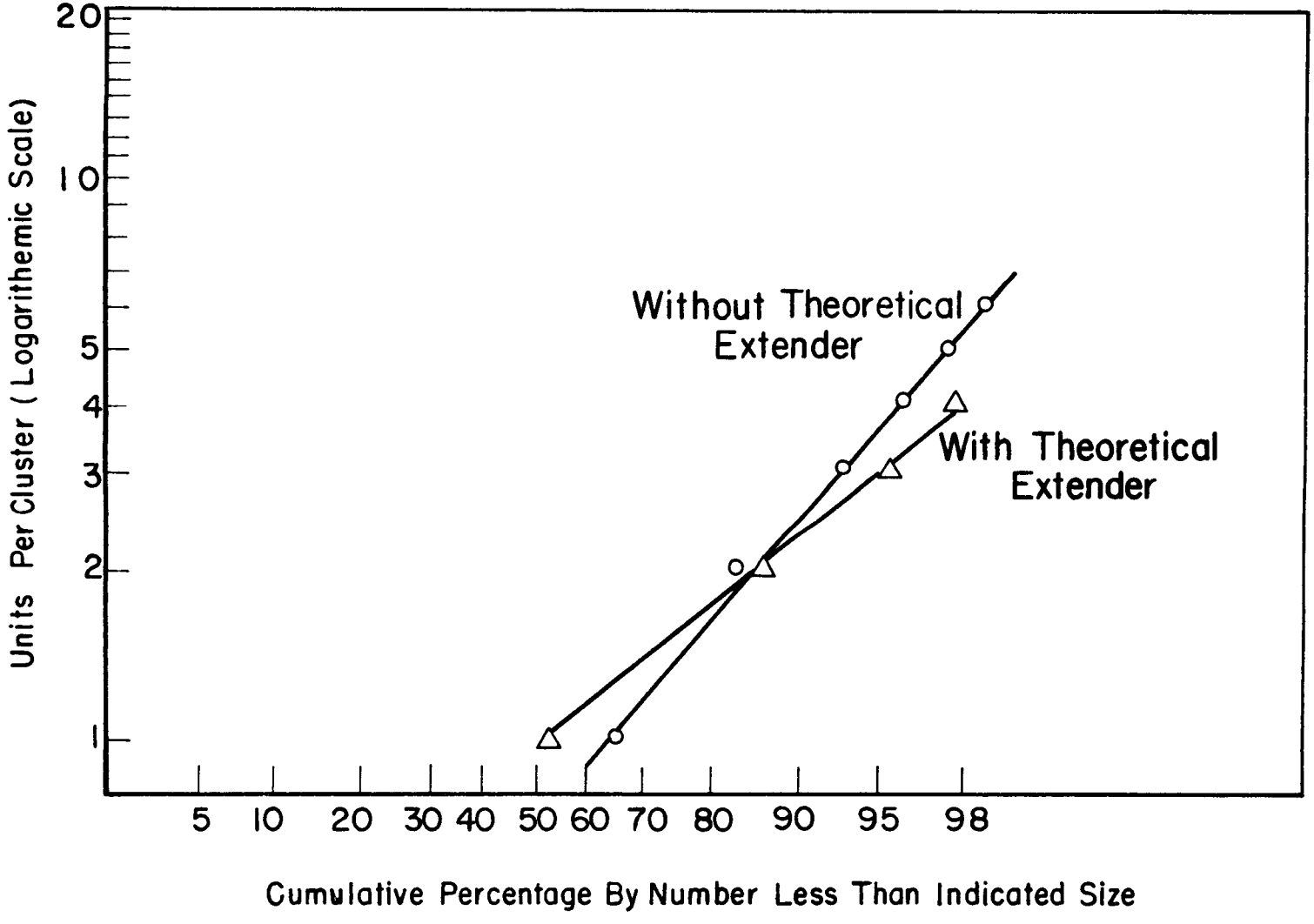


FIG. 10 SIZE DISTRIBUTIONS OF CLUSTERS FORMED FOR 0-10 VOLUME CONTENT OF IDEALIZED MONOSIZED PIGMENT DISPERSED WITH AND WITHOUT THEORETICAL EXTENDER

deposition of particles from a cloud. For this interpretation the grid becomes the surface of the filter or slide, and the overlapped particles are literally those which deposit on positions already occupied. From this point of view the total number of pairs of coordinates represents the number of particles deposited and the number of squares blocked out represents the apparent particle density.

It has been shown that the overlap losses conform to the equation

$$\log \frac{I_T}{I_0} = N + A \qquad (4)$$

But $I_T/I_0 = \alpha$, the fractional area covered, and N is the total number of coordinates considered. If all coordinates had been plotted, then N/X, where X is the total possible number of plotting positions, would be the real fractional coverage. No overlapping occured. Therefore the relationship shown in Equation 6 would seem to describe the overlap loss correction factor, since $\alpha$ is the measured quantity and $\beta$ is the corrected value where D is a constant.

$$\log \alpha = \beta + D \qquad (6)$$

A second important implication from the Monte Carlo studies concerns the nature of the cluster buildup. It was recently suggested that any reports that the particle-size distribution of particles deposited on a flat surface followed the log-normal distribution should be treated with caution, since random

juxtapositioning of particles gave rise to apparent clusters whose sizes were distributed log-normally.[4]

The evidence on which this suggestion was based was a preliminary study of patterns formed by plotting random crosses within a grid system. The growth of clusters on the grid in the Monte Carlo plotting is further evidence that random juxtapositioning of particles can give rise to apparent clusters that can be described by the log-normal distribution. The cluster distributions at various fractional densities of coverage are listed in Table 5. If the cumulative undersize distribution of the clusters is plotted on logarithmic probability paper, a straight-line relationship within the limits of statistical fluctuations is obtained. This further strengthens the theory that a deposit from a monosized cloud can appear to be from a log-normally size distributed cloud just from statistical fluctuations in deposition location.

The distributions at 10 and 20% coverage are plotted in Figure 11. Note that in the case of $\alpha = 0.2$, i.e., 20% coverage, 95% of the data are described by the log-normal distribution. It is probable that the divergence from the theoretical distribution for the remaining 5% of the data arises from the fact that these data are based upon information on a small number of

---

[4]Kaye, B.H., "Statistical Problems in Measuring the Concentration of Particles Retained on a Membrane Filter," paper presented at the Annual Meeting of the Air Pollution Control Association, Canada, June 1965.

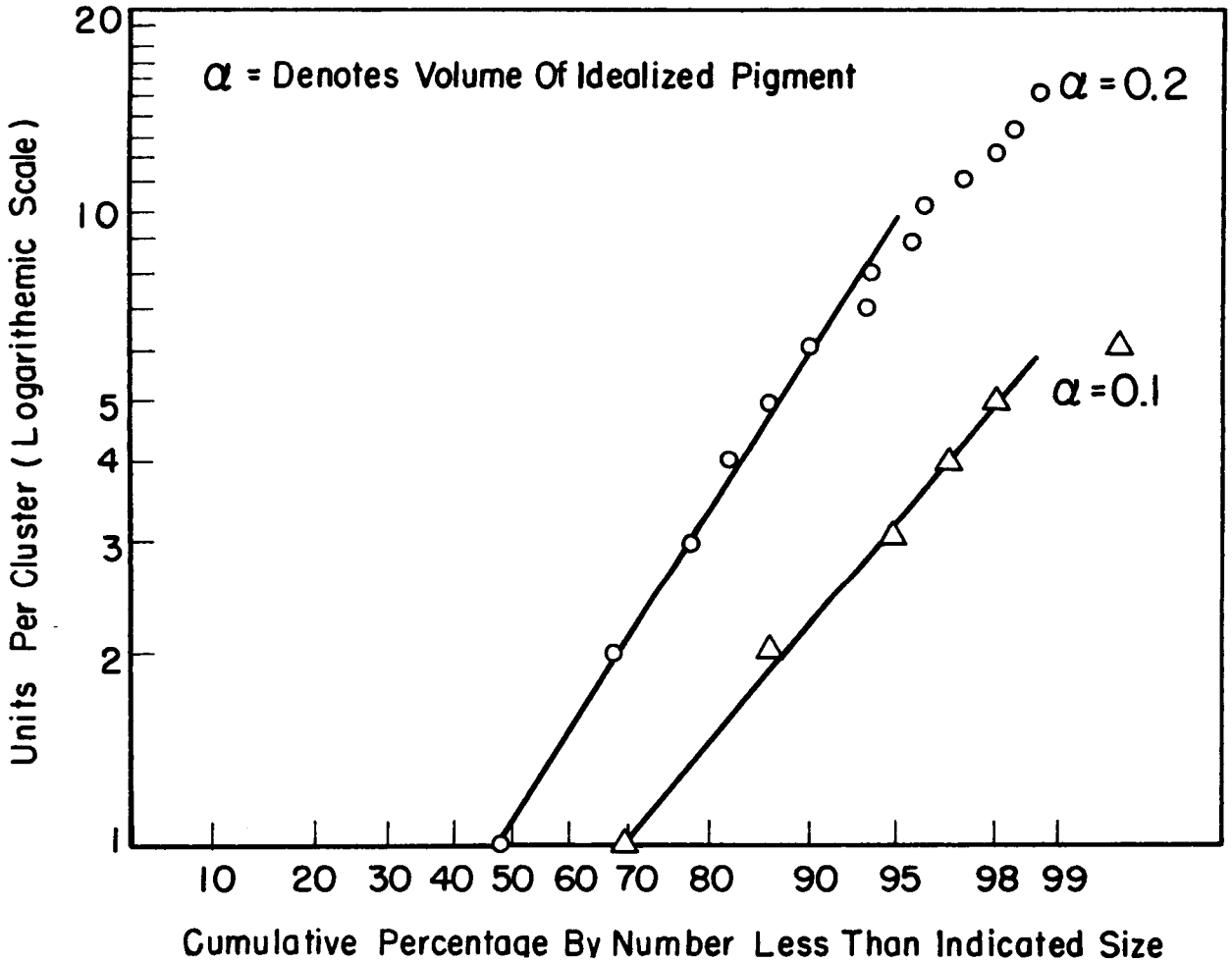


FIG. II SIZE DISTRIBUTIONS OF CLUSTERS FORMED IN BLOCK PLOTTING EXPERIMENTS

events. The data for the remaining 5% in fact are based upon nine clusters; this represents 2% of all bits of information considered when calculating the size distribution.

## III. SPECIFICATION OF PIGMENT SIZE

When attempting to predict the light-scattering properties of a paint film, the particle-size distribution of the pigment of interest is the effective distribution in the film (Report No. IITRI-C6018-14). Discussions of analytical techniques for studying the particle-size distribution of a dispersed three-dimensional system from two-dimensional sections are almost nonexistent in the literature. Thus, the work described below was initiated to examine the feasibility of developing techniques for measuring the size distribution of a pigment from sections through a paint film.

### A. Theoretical Development

Apparently some theorems in geometrical probability can be used to determine a basis for the analysis of the particle-size distribution of a pigment embedded in a paint film.

Consider n particles of arbitrary shape embedded in unit volume. The average surface, a, is defined by:

$$a = \frac{\sum_{i=s}^{i=\ell} n_i a_i}{n} \qquad (7)$$

where $n_i$ denotes the number of particles of area $a_i$, and $i=s$ and $i=\ell$ are the smallest and largest particles present.

The average volume is defined by:

$$v = \frac{\sum_{i=s}^{i=\ell} n_i \, v_i}{n} \tag{8}$$

where $n_i$ denotes the number of particles of volume $v_i$.

Let a plane section be taken at random through the pigmented matrix. Let $n_p$ be the number of sections exposed in the plane per unit area, and let $P_a$ be the average perimeter of these sections defined by the relationship.

$$P_a = \frac{\sum_{i=s}^{i=\ell} n_i \, P_i}{n_p} \tag{9}$$

where there are $n_i$ particles of perimeter $P_i$. The average area of the exposed sections is defined by:

$$A_p = \frac{\sum_{i=s}^{i=\ell} n_i \, A_i}{n_p} \tag{10}$$

where there are $n_i$ exposed sections of area $A_i$.

Now draw a random line on the exposed section. Let there be $n_\ell$ intersections with the exposed portion of pigment per unit length of the random line. The average length of the sections of the random line in the pigment particles is defined by:

$$L_\ell = \frac{\sum_{i=s}^{i=b} n_i L_i}{n_\ell} \tag{11}$$

where i=b denotes the largest intercept that has occured. In Equations 7 through 11 it is presumed that the summation is itself averaged out over a unit area and many unit lengths.

It can be shown[5] that the above defined quantities are linked by the relationship:

$$n_p A_p = n_\ell L_\ell = n v \tag{12}$$

From this relationship it follows that, since nv is the volume fraction of pigment $\alpha$, and from the definitions of $A_p$ and $L_p$

$$\alpha = \sum_{i=s}^{i=\ell} n_i A_i = \text{surface of exposed pigment per unit area} \tag{13}$$

$$= \sum_{i=s}^{i=b} n_i L_i = \text{fractional density of exposed pigment on any random line drawn on the section.} \tag{14}$$

---

[5]Kendall, M. G. and Moran, P. A. P., "Geometrical Probability," Griffins Statistical Monograph & Course No. 10, Hafner Publications Co., New York, p. 90, 1963.

Since Equations 13 and 14 would apply separately to different pigments present, the relative proportions of the different substances can be deduced by repeated application of equations. This fact is already being used in grain analysis of metal sections and in evaluation of ores; usually Equation 14 is used. The same relationship is also used to evaluate the proportion of different kinds of trees in a forest from aerial photographs.

The total perimeter per unit area, $n_p P_a$, is given by Equation 15, when averaged over many events.[6]

$$n_p P_a = \frac{2n_\ell}{\pi} \tag{15}$$

This relationship was first derived by Cauchy. A second theorem of Cauchy's shows that

$$n a = 4 n_\ell \text{ unit-length units} \tag{16}$$

(At first this equation appears to be dimensionally incorrect, but a is the average area per unit volume and is measured dimensionally in length units.)

---

[6]Steinhaus, H., Akad d. wiss. Leipzig Ber., 82, 120-130, 1930.

From Equations 12 and 16 it follows that

$$\frac{na}{nv} = \frac{4\ n_\ell}{n_\ell L_\ell} = \frac{4}{L_\ell} \tag{17}$$

This relation can be written in a more useful form:

$$\frac{S}{V} = \frac{4}{\beta} \cdot \tag{17a}$$

This important relationship can be expressed as follows: "the ratio of volume to surface per unit volume of a pigment is the average fractional length within the pigment of a random line drawn across a section through the paint film."

As far as we are aware, this form of this relationship has never been suggested for application to the study of paint films. It has been used by Bates and Pillow,[7] who showed that the average path of a sound wave in an auditorium is 4 $V.S^{-1}$, and it appears to have great potential for the study of random paths through nonhomogeneous systems.

Although we are proposing currently to use the relationship to determine the surface-to-volume ratio of a pigment, it can be used in reverse to predict the average path through a given phase in a nonhomogeneous system if the surface-to-volume ratio is known. For instance, consider the path of a drill through

---

[7] Bates, A. E., and Pillow, M. E., "Mean Free Path of Sound in an Auditorium" Proc. Phys. Soc., 59, 535-541, 1947.

a sintered metal body. If the surface-to-mass ratio of the sintered metal constituent particles were known, the average depth of actual metal in any drilled hole could be predicted.

Apart from the work of Bates and Pillow, we are not aware of any experimental proof of Equation 17. We plan to use a simulated system to test the relationship.

Again, from Equation 12,

$$A_p = \frac{n_\ell L_\ell}{n_p}$$

but, from Equation 7,

$$n_\ell = \frac{n_a P_a \pi}{2}$$

$$\therefore A_p = P_a L_\ell \frac{\pi}{2} \qquad (18)$$

It is difficult to be certain that this is the first time this relationship has been deduced, because the search for information on abstractions of this kind has to be conducted over such a broad range of the literature.

Again, by using the symbol $\beta$ for the average as the average perimeter per unit section, Equation 18 can be written in the concise form:

$$\alpha = \gamma\beta \cdot \frac{\pi}{2} \qquad (19)$$

since from Equation 13 the volume fraction of pigment is numerically the same as the area exposed per unit section.

B. Discussion

In the investigation of a possible means of deducing the properties of a three-dimensional, two-phase system from a study of two-dimensional sections, relationships relating the properties of the exposed sections of the dispersed phase to the volume-to-surface ratio of the powder and the volume concentration of the dispersed phase have been deduced. Possible limitations on the general validity of the equations for re-entrant figures are being explored. Further investigations are being pursued to determine whether size distribution of the dispersed system can be deduced from the properties of the random sections.

## IV. OPTICAL EXPERIMENTS

In an attempt to experimentally confirm our theoretical treatment of the light-scattering mechanisms in paint films, effort has been directed toward developing a simple optical system for measuring the intensity of light scattered and transmitted by particulate systems.

The optical properties of mixed powders have been briefly examined to demonstrate the validity of the optical system and to investigate its characteristics.

Further studies of the optical properties of two-component dispersed systems of various compositions and thicknesses will be made, and the results will be compared with those obtained theoretically for randomly superimposed screens.

### A. Description of the Apparatus

A vertically mounted optical bench (Figure 12) is used to support a mercury lamp and diffuser directly above a sample holder. The light scattered and transmittted at any angle in a plane perpendicular to the sample surface is detected by a photo resistive cell that can be rotated in a circle about the sample. The light intensity is monitored on an oscilloscope as a change in the DC voltage developed across a resistance in series with the photocell.

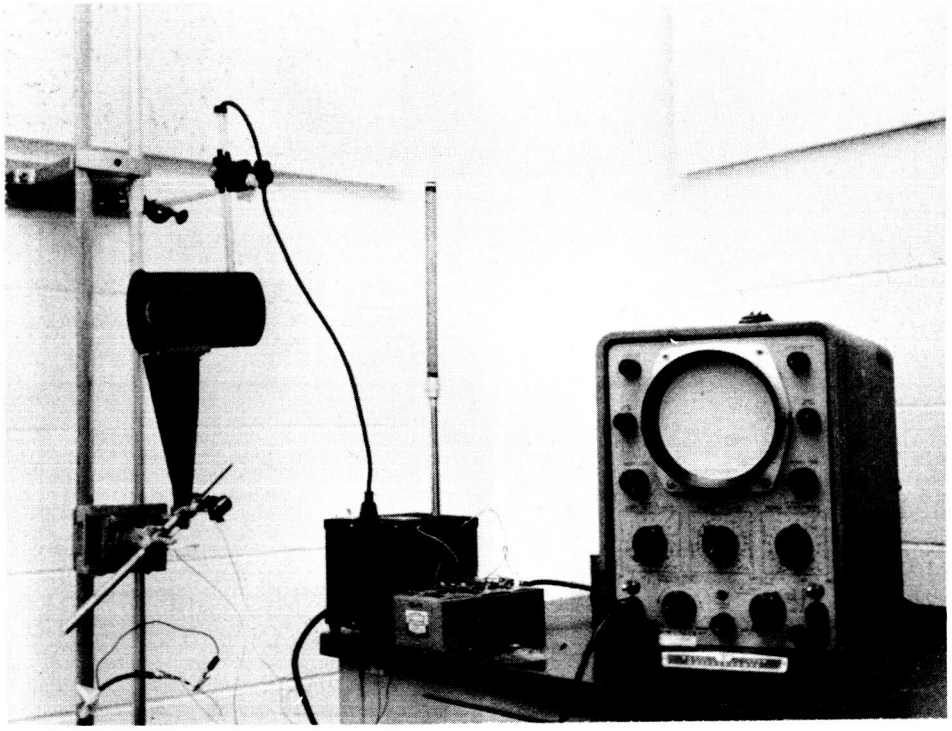

Figure 12

OPTICAL BENCH REFLECTOMETER

Figures 12 and 13 show the apparatus; Figure 14 is a schematic diagram of the detection circuit.

## Preparation of Powder Samples

Initial attempts to make a mixture of carbon black and titanium dioxide by grinding produced a lumpy powder of uneven surface texture. Examination showed that the powder composition was not constant throughout the lumps. The lumps were broken up and passed through a U.S. Standard Sieve No. 325 to give a fine powder. However, this powder agglomerated rapidly when powder beds were made, giving gross surface roughness.

Thus, it was considered impossible to obtain a constant surface texture and a uniform mixture by dry powder mixing alone. The method established in the paint industry in which the powder mixture is pressed against a plate that is subsequently removed was rejected because of the unknown pressure gradient and manner of packing immediately adjacent to the plate, which could affect the reflectance properties of the surface.

An alternative method has been devised in which liquid suspensions of the component to be mixed are combined and filtered onto a membrane filter (Millipore HA Series). The deposits have an even surface texture and color as determined by visual examination.

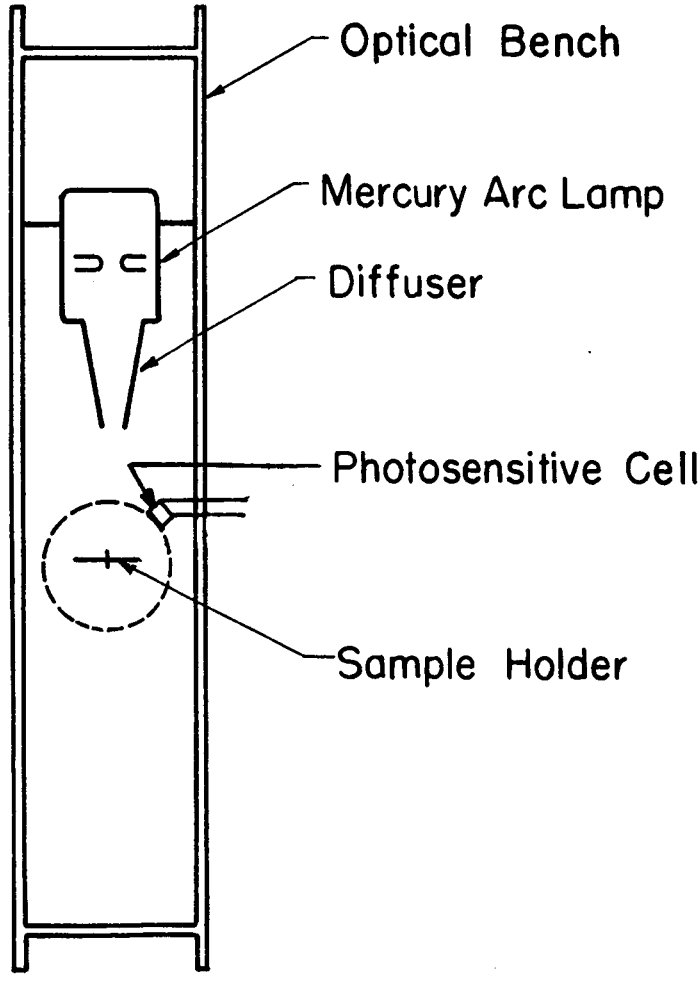


FIG.13 SCHEMATIC DIAGRAM OF THE REFLECTOMETER

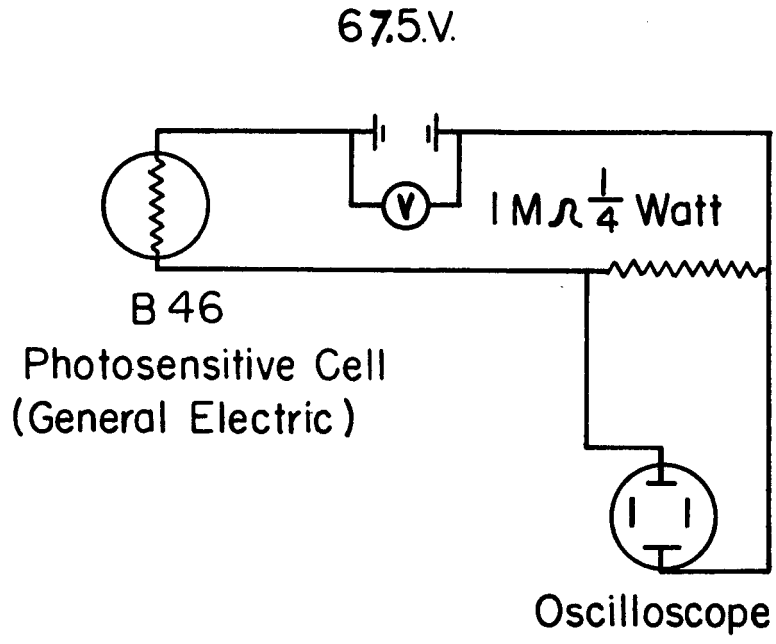


FIG. 14 SCHEMATIC DIAGRAM OF THE DETECTION CIRCUIT

The following results were obtained by using samples prepared in this manner. To further develop this technique, the possible loss of very fine particles when the suspension is filtered will be investigated.

## C. Experimental Results

A series of known volumes of 0.1% by weight aqueous titanium dioxide suspension was deposited on separate white membrane filters. The dried filters were examined by using the photocell placed at 10° intervals from 20 to 90° to the vertical. The results are shown in Table 7. Note that the reflected light intensity remains essentially constant for deposits of 1 cc and larger.

Table 7

REFLECTION FROM TITANIUM DIOXIDE ON WHITE FILTER

| Angle, ° | Reflection from Filter Alone | Reflection, Volume of 0.1% Titanium Dioxide Suspension, cc | | | | |
|---|---|---|---|---|---|---|
| | | 0.1 | 0.25 | 0.5 | 1.0 | 2.0 |
| 20 | 90 | 80 | 77 | 78 | 74 | 74 |
| 30 | 82 | 69 | 68 | 69 | 67 | 66 |
| 40 | 72 | 58 | 58 | 58 | 57 | 57 |
| 50 | 60 | 46 | 50 | 46 | 48 | 48 |
| 60 | 46 | 36 | 38 | 33 | 36 | 36 |
| 70 | 31 | 27 | 24 | 20 | 23 | 25 |
| 80 | 16 | 13 | 13 | 13 | 11 | 13 |
| 90 | 7 | 5 | 4 | 2 | 5 | 5 |

Since the reflectivity of the filter and the powder are similar, further measurements were made by using black filters. The results shown in Table 8 are those obtained from observations on damp and dry filters.

Table 8

REFLECTION FROM TITANIUM DIOXIDE ON BLACK FILTERS

| Angle, ° | Reflection from Filter Alone | Reflection, Volume of 0.1% Titanium Dioxide Suspension, cc | | | | | | | |
|---|---|---|---|---|---|---|---|---|---|
| | | 0.1 | 0.25 | 0.5 | 1.0 | 2.0 | 3.0 | 5.0 | 10.0 |
| | | Damp Filters | | | | | | | |
| 20 | 18 | 24 | 33 | 38 | 48 | 53 | 54 | 58 | 60 |
| 30 | 17 | 21 | 31 | 36 | 47 | 52 | 52 | 54 | 59 |
| 40 | 16 | 20 | 28 | 32 | 42 | 47 | 47 | 49 | 52 |
| 50 | 13 | 17 | 24 | 26 | 38 | 39 | 40 | 44 | 44 |
| 60 | 12 | 13 | 20 | 20 | 30 | 32 | 33 | 36 | 36 |
| 70 | 9 | 10 | 15 | 16 | 24 | 24 | 23 | 26 | 25 |
| 80 | 6 | 6 | 9 | 10 | 14 | 10 | 14 | 16 | 15 |
| 90 | 3 | 2 | 3 | 3 | 3 | 2 | 2 | 6 | 6 |
| | | Dry Filters | | | | | | | |
| 20 | | 35 | 45 | 46 | | 60 | 60 | 63 | 62 |
| 30 | | 32 | 39 | 40 | | 56 | 58 | 60 | 60 |
| 40 | | 29 | 33 | 37 | | 51 | 51 | 60 | 59 |
| 50 | | 24 | 31 | 32 | | 41 | 42 | 48 | 47 |
| 60 | | 20 | 26 | 24 | | 32 | 33 | 38 | 38 |
| 70 | | 15 | 19 | 81 | | 25 | 25 | 25 | 26 |
| 80 | | 9 | 12 | 11 | | 17 | 16 | 16 | 15 |
| 90 | | 3 | 3 | 4 | | 6 | 6 | 5 | 6 |

A series of graphite and titanium dioxide mixtures was deposited on white filters and observations were made as previously. The results obtained are shown in Figure 15, in which the intensity of the light reflected at 20° is plotted against the weight percent graphite in the sample.

The particle-size distributions of graphite and the titanium dioxide suspensions have been determined; the average particle sizes were 0.8 and 1.0 $\mu$, respectively. More detailed particle-size information will be obtained, if necessary, by using a centrifugal photosedimentometer.

D. Discussion

Samples deposited on both black and white filters show a constant intensity of reflected light for sample volumes greater than about 2 cc (Tables 7 and 8). Thus, all forward-directed light is scattered in penetrating a film of the thickness corresponding to 2 cc.

If we assume a monosized powder of packing fraction 50%, a 2-cc sample will form a deposit about 10 particles deep. This compares well with the theoretical work previously reported (Report No. IITRI-C6018-15), in which seven screens of packing fraction 50% transmitted less than 1% of the forward beam. This finding suggests that when the foreward beam is destroyed, the resultant energy is present as diffuse radiation.

Tables 7 and 8 show that the intensity of the reflected light decreases as the angle of the photocell to the vertical is increased. If this were purely a geometrical effect, the

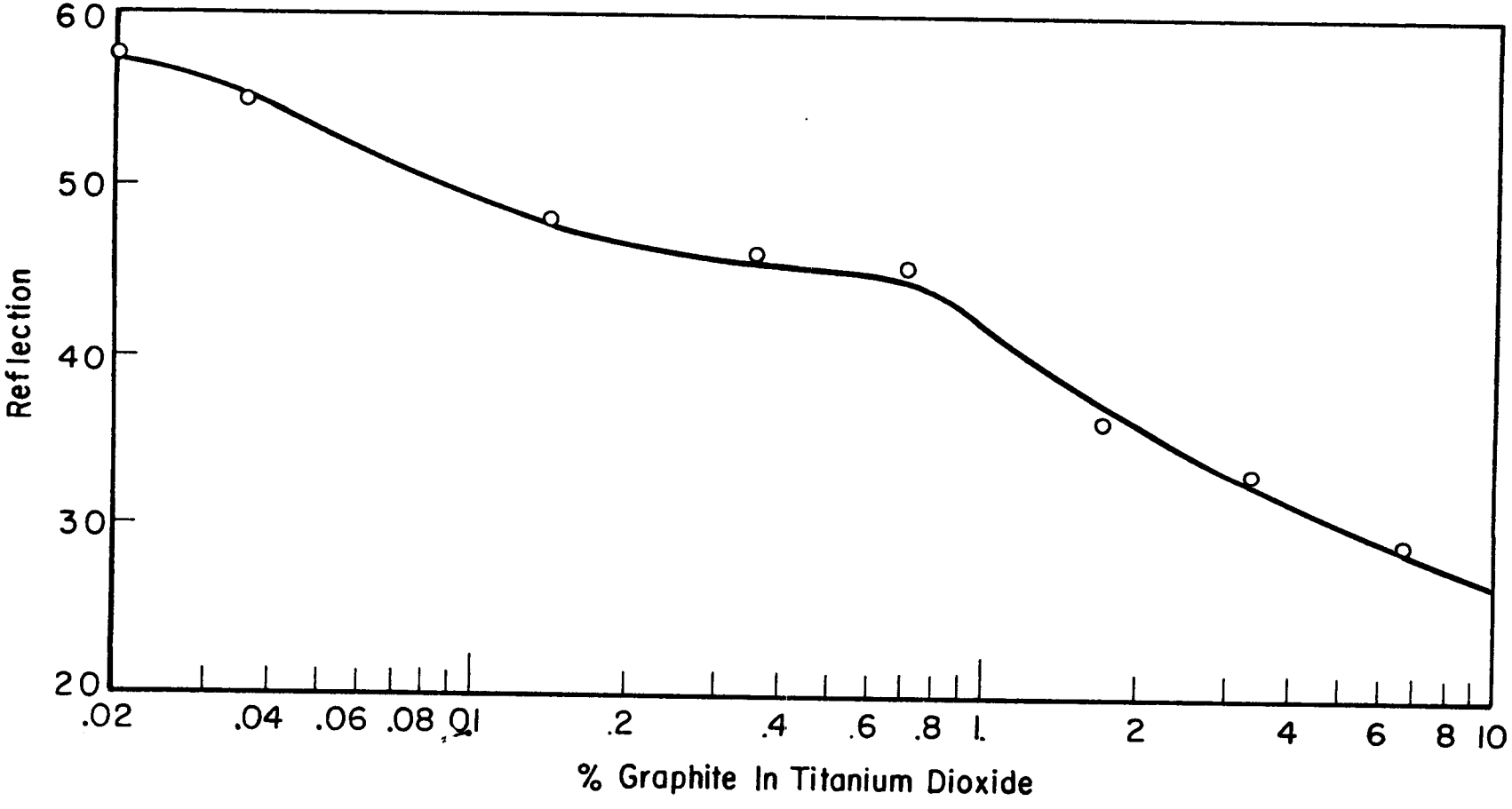


Fig. 15 REFLECTANCE OF RUTILE AND GRAPHITE MIXTURES ON A NOMINALLY WHITE SURFACE

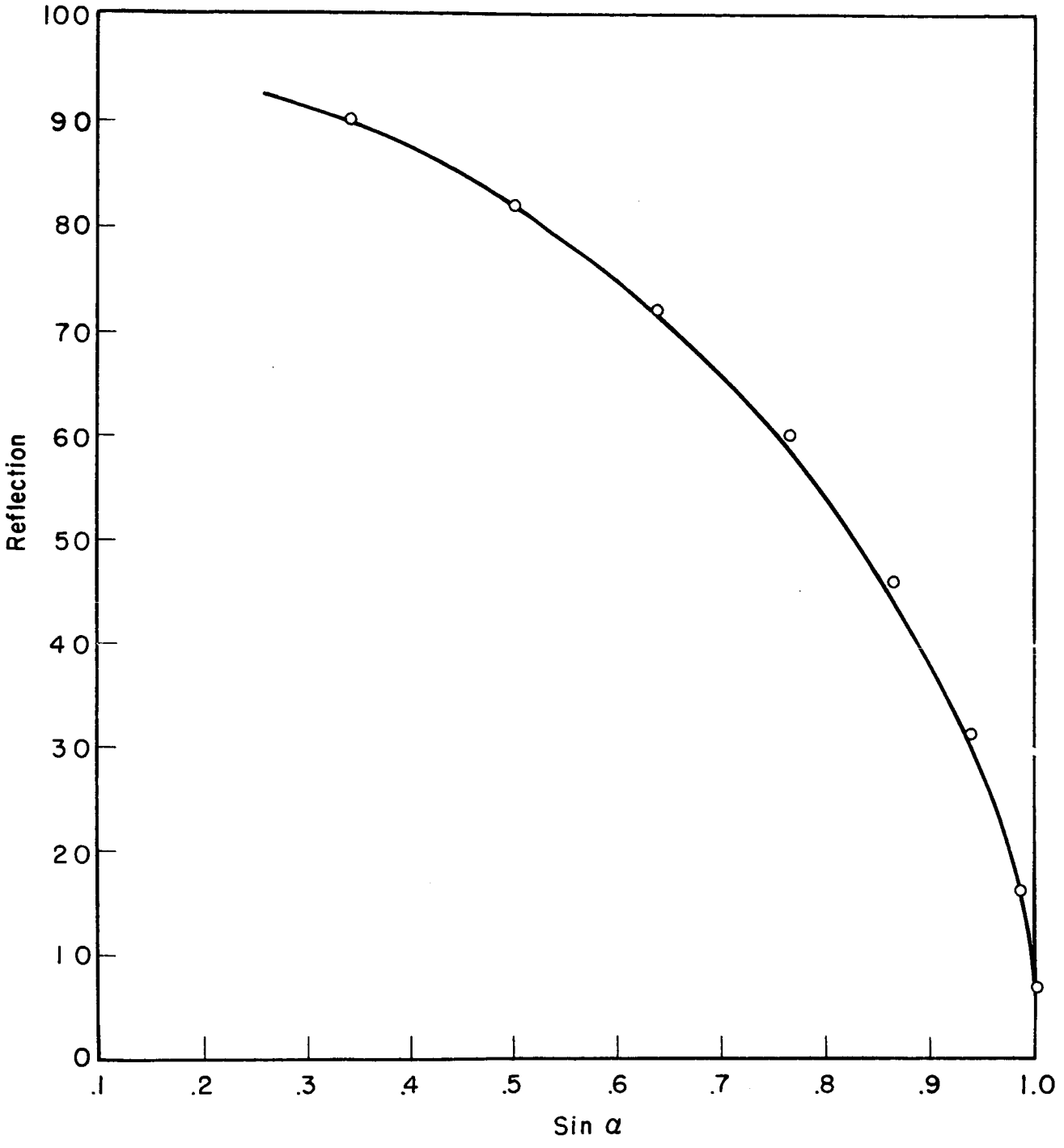


FIG. 16 RELATIONSHIP BETWEEN ANGLE $\alpha$ OF PHOTOCELL AND VISIBLE AREA OF DEPOSIT

plot of intensity versus the sin of the angle would give a straight line. Figure 16, which shows a nonlinear relationship, indicates that the incident beam is collimated and the reflected beam is directional. At high angles of scatter results were susceptible to tilting and bending of the filter and deposit, presumably because of the small angle of observation. To eliminate errors resulting from these two effects, it is recommended that measurement be made only at small, known scattering angles.

Table 8 shows the results for damp and dried deposits. At high observation angles the results are not significantly different, but for angles smaller than about 40° a systematic difference is observed. Presumably, the moisture collects by capillary action within the filter and between the particles. This could have the effect that at large angles the photocell views only the tops of particles (as an observer would see mountains from the surrounding plains) and does not consider the moisture. At smaller angles the moisture in the hollows contributes to the scattering to the photocell and results in the observed differences.

Figure 16 shows a simple relationship between the concentration of black in a mixture and the intensity of reflected light. Results (not plotted) for 100% black were identical with 6% black, presumably because the intensity of light reflected from the crystal faces of the graphite flakes is comparable with that scattered by the less crystalline white titanium dioxide.

It is thought that the discontinuity of Figure 16 may be due to differences in texture of the titanium dioxide and graphite. Further work will be conducted by using carbon black that is more absorbing and less reflecting than graphite.

## F. Further Work

Further work will be directed at gaining an understanding of the mechanisms of scattering in paint films from studies of the reflectance and transmission of dispersed solids systems having a range of absorbing solids content.

Distribution List:

| Copy No. | Recipient |
|---|---|
| 1-25 + reproducible | National Aeronautics & Space Administration<br>Office of Grants and Research Contracts<br>Washington, D. C. |
| 26 | Mr. J. J. Gangler<br>National Aeronautics & Space Administration<br>Office of Advanced Research and Technology<br>Washington 25, D. C. |
| 27-30 + reproducible | Mr. D. W. Gates (M-RP-T)<br>George C. Marshall Space Flight Center<br>Huntsville, Alabama |
| 31 | Mr. Conrad Mook<br>Code RV<br>National Aeronautics & Space Administration<br>Washington, D. C. |
| 32 | Mr. William F. Carroll<br>Jet Propulsion Laboratory<br>4800 Oak Grove Drive<br>Pasadena, California |
| 33 | Mr. Sam Katzoff<br>National Aeronautics & Space Administration<br>Langley Research Center<br>Langley Field, Virginia |
| 34 | Mr. Joseph C. Richmond<br>National Bureau of Standards<br>Washington, D. C. |
| 35 | Mr. James Diedrich, Mail Stop 7-1<br>Lewis Research Center<br>Cleveland, Ohio |
| 36 | IIT Research Institute<br>Division U Files |
| 37 | IIT Research Institute<br>Editors, J. J. Brophy, Main Files |
| 38 | IIT Research Institute<br>J. I. Bregman |
| 39 | IIT Research Institute<br>B. A. Murray |

Distribution List (cont.)

| Copy No. | Recipient |
|---|---|
| 40 | IIT Research Institute<br>Y. Harada, Division G |
| 41 | IIT Research Institute<br>J. E. Gilligan, Division U |
| 42 | IIT Research Institute<br>S. Katz, Division C |
| 43 | IIT Research Institute<br>B. Kaye, Division C |
| 44 | IIT Research Institute<br>V. Raziunas, Division C |
| 45 | IIT Research Institute<br>M. Jackson, Division C |
| 46 | IIT Research Institute<br>G. A. Zerlaut, Division C |